Prediction of Tubular Projectile Aerodynamics Using the ZEUS Euler Code

J. Evans*
Defence Research Establishment Valcartier, Quebec, Canada
and
A. B. Wardlaw†
Naval Surface Warfare Center, White Oak, Maryland

A subcaliber spinning tubular projectile was developed as a range-limited training ammunition for rifled tank guns, providing a ballistic match with the kinetic-energy-penetrator round. The supersonic shock-swallowed aerodynamics of the tubular projectile were obtained from wind-tunnel and free-flight experiments, extended linear theory, and subsequently the ZEUS Euler code. This paper presents a summary of results and makes comparison between experimental results and ZEUS for the cases of the subcaliber tubular projectile, the Royal Aircraft Establishment tubular inlet, and the National Aeronautical Establishment tubular projectile—Model A. The Euler code matched tunnel results for the subcaliber tubular projectile as follows: $C_{N\alpha}=10\%$, $C_{m\alpha}=15\%$, and the center of pressure position X_{cp} to within 0.2 diam. Shock/boundary-layer interactions were shown to move the internal shock reflection points slightly ahead of the positions calculated by the inviscid ZEUS code; however, the net effect of this was small because of the dominance of the external forces on the tube. Pressure-contour maps display internal and external flowfields in axial and crossflow planes, and internal pressure contours matched experimental data well.

Nomenclature

A = axial force
C_A = axial-force coefficient = $A/(QS)$
C_m = pitching-moment coefficient = $m/(QSd)$ (about c.g.)
$C_{m\alpha}$ = pitching-moment coefficient slope at $\alpha = 0$
C_N = normal-force coefficient = $N/(QS)$
$C_{N\alpha}$ = normal-force coefficient slope at $\alpha = 0$
C_p = pressure coefficient = $(p\text{-}p_\infty)/Q$
d = external body diameter (and reference length)
d_i = inlet diameter
d_t = throat diameter
l = total tube length
M = Mach number
m = pitching moment about c.g.
N = normal force
p = pressure
Q = dynamic pressure = $\frac{1}{2}p_\infty V^2$
r = internal radius = $d_t/2$
S = reference area = $(\pi/4)d^2$
V = velocity
X_{cp} = center of pressure position at $\alpha = 0$ (body diameters ahead of base)
x = distance aft of nose
α = angle of attack
β = $\sqrt{M^2-1}$
θ_e = external wedge angle
θ_i = internal wedge angle
ρ = density
ψ = circumference angle

Subscript
∞ = ambient conditions

Received Nov. 4, 1988; presented as Paper 89-0334 at AIAA 27th Aerospace Sciences Meeting, Reno, NV, Jan. 9-12, 1989; revision received Feb. 27, 1989.

*Defense Scientist, Armaments Division.
†Aerospace Engineer, Applied Mathematics Branch. Associate Fellow AIAA.

Introduction

A SUBCALIBER spinning tubular projectile has been developed for use as a limited-range target-practice round for the 105-mm rifled tank gun. This work resulted from a requirement for a projectile having a ballistic match with the kinetic-energy penetrator service round (APFSDS) to a range of 3 km, with a maximum range of 8 km when fired at a gun elevation of 10 deg. The tubular-projectile concept is ideally suited for this application because of the large variation of its drag coefficient with Mach number. Distributing the mass of a projectile in the form of a thin tube reduces the supersonic wave drag. For a properly designed projectile at high supersonic launch velocities, the core flow becomes supersonic at the gun muzzle and the drag coefficient is low, making it possible to fly a long, flat trajectory similar to that of the arrow-shaped APFSDS. As the tubular projectile decelerates, however, it reaches a Mach number where the throat cannot pass all of the flow that the inlet swallows and the tube chokes (i.e., a shock wave is expelled and stands as a bow shock in front of the tube). The drag coefficient in the shock-expelled regime is substantially higher. In the case of the subcaliber tubular projectile, early experimental work showed that a projectile with the necessary geometry to achieve a ballistic match with APFSDS required an effect to supplement choking to achieve the desired maximum range, and thus spin-damping fins were introduced. The hollow projectile was still required for its low drag. The fins reduce the spin to the point where the projectile becomes gyroscopically unstable at a predetermined range, leading to large angles of attack, choking, and high drag. Subsequent experimental firings have suggested that spin damping is the primary range-limiting mechanism; however, choking prevents a return to low-drag stable flight, and so remains a desirable feature.

The supersonic shock-swallowed aerodynamics of the shape were obtained from tunnel and free-flight tests together with linear theory and later using the ZEUS Euler code. The aerodynamic coefficients for this initial flight regime determine the projectile stability and trajectory match with APFSDS, and an understanding of the flowfield is thus critical to the design of the round. This paper describes the experimental test results and compares them with ZEUS, which was then applied to the RAE and NAE tubular models for further verification of results. No choked-flow cases were treated in this paper, as ZEUS only computes flowfields that are everywhere supersonic.

Background

Experiments

References to experimental work on tubular projectiles are numerous, with the earliest dating from 1858 describing firings of hexagonal-shaped hollow bodies.[1] Reference 2 cites firings in 1894 and references tests at Ballistic Research Laboratories (BRL) done in 1944 on 20-mm shells. Experimental research on tubular projectiles started at the Defence Research Establishment Valcartier (DREV) in the early 1970's with free-flight range testing by Laviolette et al.[3] A summary of information on tubular-projectile internal flows was made by D'Souza and Laviolette.[4] Research eventually led to the development and production of the full-bore spinning tubular projectile (STUP) 105-mm training ammunition representing an earlier generation of higher-drag tank ammunition (APDS) described in Ref. 5. This STUP relies entirely on choking to achieve its range performance. In support of the development, extensive wind-tunnel tests were conducted at NAE by Atraghji[6-7] on three configurations of tubular projectile with l/d_t ratios from 3 to 4 at Mach numbers from 0.8 to 4.0 (l/d_t is defined as the total tube length l divided by the diameter of the parallel throat section d_t and is an important parameter for internal flow calculations, being related to the number of shock reflections). Circular inlets were studied experimentally at RAE by Roe[8] for models having l/d_t ratios of 4.6–6.9 at a Mach number of 4 and angles of attack up to 20 deg; and by Cook[9,10] for tubes with l/d_t ratios of 1.4, 2.8, and 4.2 at Mach numbers 1.4–2.2 and low angles of attack. Reference 11 describes wind-tunnel and range tests conducted at Edgewood Arsenal and BRL on several configurations of projectile, leading onto a concept known as a tubular convergent/divergent projectile and preliminary development of a projectile for use with the 20-mm Vulcan gun system. In the 1980's, tunnel tests on ball-obturated projectiles were conducted by Nunn and Bloomer[12] of the U.S. Naval Postgraduate School and also by Nunn and Bry.[13] Evans at al.[14-16] conducted tunnel tests at DREV on subcaliber tubular configurations at Mach numbers from 3–4 and angles of attack up to 5 deg for a tube with an l/d_t ratio of 7.4, which are further described in this paper. The subcaliber projectile is less wind sensitive and has lower drag than its full-bore counterpart and so can match the trajectory of APFSDS. Nietubicz and Heavey[17] describe wind-tunnel tests of a tube with l/d_t at Mach 1.7 and 3.5 at zero incidence for validation of BRL's numerical work on tubular projectiles, and Danberg and Sigal[18] present tunnel results for solid-fuel ramjet projectiles (SFRJ).

Theory

The first theoretical approach to tubular projectile aerodynamics was the development of an approximate theory for the external and internal supersonic flow past a tube of nearly constant radius at small incidence. This work was done by Ward[19,20] and Lighthill[21] in the 1940's, using the Heaviside operational method applied to linear perturbation theory. The method, although adequate for short tubes, breaks down for longer tubes due to a singularity in the internal flowfield when the l/d_t value is greater than β. Roe[8] has shown that the tunnel and linear theory results diverge even before reaching this critical length. The problems associated with the tube shock swallowing and expulsion processes are those of standard supersonic inlets, well described in Shapiro[22] and Hermann,[23] and hypersonic inlet flows were studied by D'Souza et al.[24]

In 1983, Politis et al.[25] developed the ACOSTUP program to predict the aerodynamic coefficients of tubular projectiles using Ward's linear theory extended empirically to match experimental data on longer tubes. The code predicts axial and normal forces, pitch and roll moments, Magnus force and moments, and pitch damping for tubular shapes with blunt or sharp leading edges at Mach numbers from 1.5–5 and low angles of attack. Internal and external normal forces and moments are calculated using polynomial fits to the RAE data,[8] which limits the range of applicability to tubes for which l/d_t ratios are less than 2.0β. Static force, moment, and drag predictions have been validated for some short-tube configurations; however, a complete code validation has yet to be done. The code in its present form cannot deal with external fins.

In support of solid-fuel ramjet tubular projectile applications, BRL has conducted studies using numerical solutions of the thin-layer Navier-Stokes equations.[17] This work was a follow-on to a hollow projectile code[26,27] used to study ring airfoil grenades. For simple wedge-shaped configurations with $l/d_t = 3.6$ at zero incidence in choked and unchoked conditions, a qualitative agreement with tunnel data was observed from Mach 1.7–3.5. The code was applied to an SFRJ configuration at Mach 1.8 and 4.3 at zero incidence. The internal configuration was very complex and regions of separated flow were predicted to exist. Reference 18 compares results from tunnel tests on SFRJ projectiles (with a variety of internal contours at Mach 4,$\alpha = 0$) with Navier-Stokes (N-S) code results. Agreement was quite good; however, oscillatory solutions were observed.

No reference to three-dimensional numerical predictions of tubular projectile flowfields was identified in this review of the literature.

ZEUS Code Description

This paper describes the application of the ZEUS Euler code[28] to the problem of predicting tubular projectile flowfields at supersonic Mach numbers and angles of attack up to 10 deg.

The steady Euler equations are hyperbolic in regions of supersonic flow. This permits solutions to be computed from an initial data plane located near the front of a supersonic body. The ZEUS code calculates the flowfield by marching such an initial data plane down the axis of the body; however, this marching procedure is valid only if the flowfield is everywhere supersonic. Details of this computational procedure are provided in Ref. 28.

The ZEUS code integrates the Euler equations using a second-order extension of the Godunov method. The Godunov method is an upwind scheme that is based on the Reimann problem. In steady supersonic flow, the Reimann problem represents the confluence of two, two-dimensional supersonic streams as illustrated in Fig. 1. At the point of stream intersection, shocks or expansion fans form that turn both streams to a common direction. The appropriate direction is the one producing the same pressure to both streams. The two final streams need not feature the same density or velocity and a slip line generally forms between them. Solutions to the Reimann problem feature constant properties along any line passing through the point of initial stream intersection (e.g., rays A., B, and C of Fig. 1). The nonlinearity of the shock/expansion relations requires that the Reimann problem be solved iteratively. In cases where the two streams feature similar properties, a closed-form linear solution can be obtained.

The original Godunov's method[29] is first-order and is usually cast in a finite-volume form. The properties within each computational cell are assumed to be constant and fluxes at cell edges are calculated using the Reimann problem. The two sets of properties adjacent to each cell edge define the two streams making up the Reimann problem. Fluxes crossing a

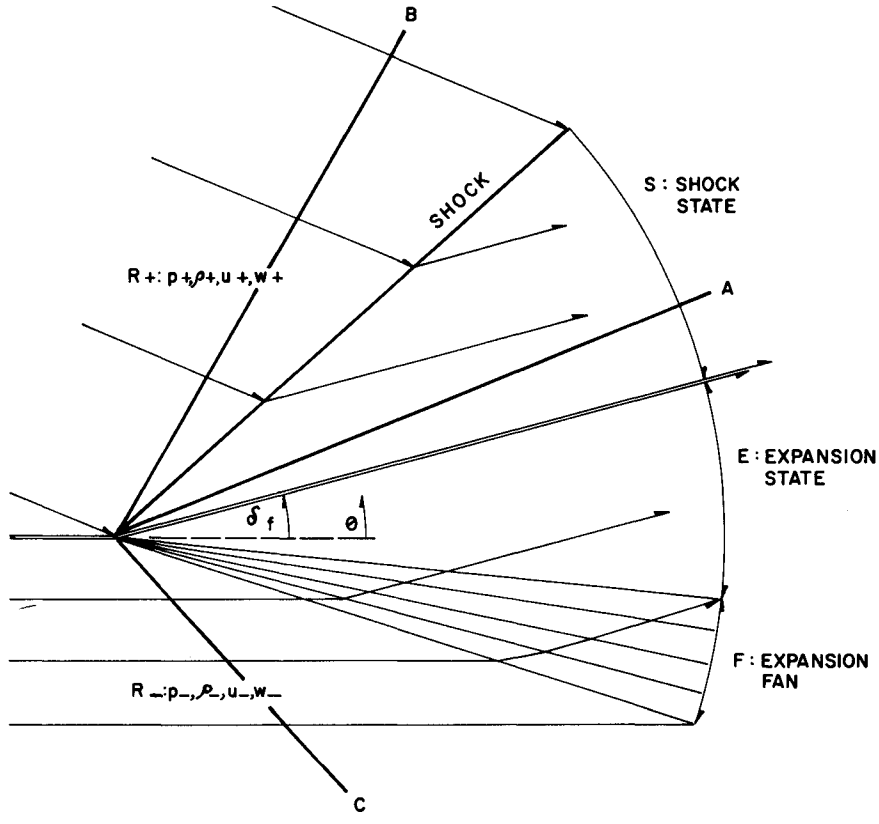

Fig. 1 Confluence of two supersonic streams—the Reimann problem.

cell edge are computed from the solution to the Reimann problem. As mentioned previously, the properties along any ray originating from the point of the initial stream intersection are constant. The properties along the ray parallel to the cell-edge orientation are used to compute the flux. When this direction falls between the shocks/expansions defining the Reimann problem (ray A in Fig. 1), the computed flux is influenced by properties at both adjacent cell edges. In other circumstances (rays B,C), which occur only when the flow normal to the edge is supersonic, the cell-edge flux will be a function of only one cell's properties. The active cell is upstream or upwind of the cell edge, reflecting the correct domain of dependence of the problem.

The Godunov method can be extended to second-order using a scheme similar to that originally suggested in Ref. 30. Second-order accuracy in the crossflow plane is achieved by assuming a linear property variation within each cell, while second-order accuracy in the marching direction is attained by adding a predictor step. At the start of each time step, the property slopes within a cell are determined by central differencing. To prevent oscillations near shocks, these slope values are limited as follows:

$$\frac{\partial f}{\partial y} = \frac{\min}{\Delta y}\left[\frac{|f_{i+1}-f_{i-1}|}{2},\ k|f_{i+1}-f_i|,\ k|f_i-f_{i-1}|\right] \text{sign}(f_{i+1}-f_{i-1})$$

Here f and y are arbitrary dependent and independent variables, respectively; the subscripts refer to grid point number in the y direction, and $1<k<2$.

The predictor step is constructed using the Euler equations in nonconservation form. The derivatives present in these equations are evaluated using the limited slopes as previously computed. In the vicinity of shock and other discontinuities, the limiter will reduce all slopes to zero and the preceding scheme collapses to the first-order Godunov method.

The technique described previously for constructing a second-order Godunov method has been applied to unsteady, compressible flow [31-33] and to two-dimensional steady supersonic flow.[34] A common element in each of these schemes is the use of limiters that reduce slope values in the vicinity of shocks and expansions; however, the specific limiter used varies extensively as does the form of the predictive step.

The grid is generated using a multiple zone approach, which entails dividing the crossflow plane into several quadrilateral zones, and applying a simple, separate transformation to each. For geometries with circular cross section, the edges of the zones are described in cylindrical coordinates, whereas in other cases rectangular coordinates are used. Zone boundaries are taken to coincide with the body, fin surfaces, or the bow shock, which can be fitted.

Internal grids on axisymmetric bodies are generated using an arbitrarily small solid centerbody. When calculating internal flowfields for tubular projectiles a centerbody radius of 0.001 body diameters was used, so that the cell face bordering this surface was so small as to present effectively zero area. At zero incidence, the centerline is a streamline, and the centerbody poses no problem; however, at incidence the presence of the centerbody could conceivably prevent flux through the centerline that otherwise would occur. The error is not expected to be large, however, as the area of the cell face in contact with the centerbody is so small as to make the cell effectively a triangle, and flux near the centerline passes through the adjacent cell faces. The starting-plane solutions were taken to be freestream conditions, and the flow was marched along the body in two separate runs for the internal and external flows, respectively. For fully supersonic flows, the two flows are completely independent.

The internal runs were conducted typically using a single zone made up of 36 cells between the centerbody and the inner wall, and 18 cells along the circumference (between $\psi=0$ and 180 deg) at each axial marching plane. The symmetry of the problem permitted an analysis of the half-body flowfield

alone. The external flow was done using a 36 × 36 mesh divided into two zones meeting at the fins. The fins were considered to have zero thickness (although ZEUS can include thick fins if desired). Finer meshes were tried but showed minimal effect on overall results. Because of the steady nature of the equations, spin effects could not be modeled. Typically, the CPU times were on the order of 250 s on a CRAY 1-S machine for internal flows, involving approximately 2000 axial steps, while external flows took 50 s, requiring 500 axial steps.

Internal flowfields featuring reflecting and intersecting shock waves can be predicted with ZEUS provided that the flow remains wholly supersonic. This implies that Mach reflections cannot exist because of the resulting normal shock wave. Mach reflections occur if the Mach number ahead of the reflection point is low or if the turning angle is large, and may occur at the tube inner wall or at the centerline (Mach disc). ZEUS could predict the formation of a Mach disc or Mach reflection, but the calculation would stop at that point. This limits its range of application to higher Mach numbers and smooth geometries.

Results

Subcaliber Tubular Projectile

The tubular model tested in the DREV wind tunnel (see Ref. 15 for details) is shown in Fig. 2, and represents an early version of the final production projectile. The model was supported in the tunnel using a swept strut connected to a balance attached to a curved sting. A windshield surrounded the balance and strut so that the balance elements sensed only the forces on the model. Figure 3 shows the model/strut assembly in position in the DREV 0.6 × 0.6-m trisonic indraft tunnel. Many tests were conducted using an Army/Navy Spinner calibration model in order to verify that the strut mount did not interfere with the aerodynamics of the projectile. Comparing published Spinner data[35-36] with DREV tunnel data obtained using a Spinner Model the same diameter as the tubular model, the accuracy of the tubular projectile aerodynamic coefficients obtained with the strut mount were determined to be as follows: $C_{N\alpha} = 6\%$, $C_A = 10\%$, and $X_{cp} = 0.2$ diameter and $C_{m\alpha} = 15\%$, for Mach numbers above 3.0. Precision of tunnel results have been estimated as follows: $C_{N\alpha} = \pm 5\%$, $C_A = \pm 3\%$, $X_{cp} = \pm 0.2$ diam and $C_{m\alpha} = \pm 4\%$, because of run-to-run scatter caused by flow nonuniformity and model vibration. Accuracy is defined as the difference between the mean of multiple runs and the known result for Spinner, where a positive number indicates a higher value of the tunnel result. The tunnel thus overestimated all parameters. At lower Mach numbers (< 2), shocks off the conical windshield of the strut impinged on the model and created large interference. The best results were obtained at positive angles of attack when the strut was on the leeside of the model. Force and moment coefficients were obtained by using a linear best fit through the tunnel data. Tests were done at the Mach numbers 3.0, 3.5, and 4.0. It was not possible to conduct spin tests on the model; however, free-flight trials were used to measure spin damping and drag coefficients and base drag was measured in the tunnel using an annular base-pressure tube.

Figures 4–6 present the aerodynamic coefficients and show the comparison with ZEUS calculations for $\alpha = 1$ deg. Overall

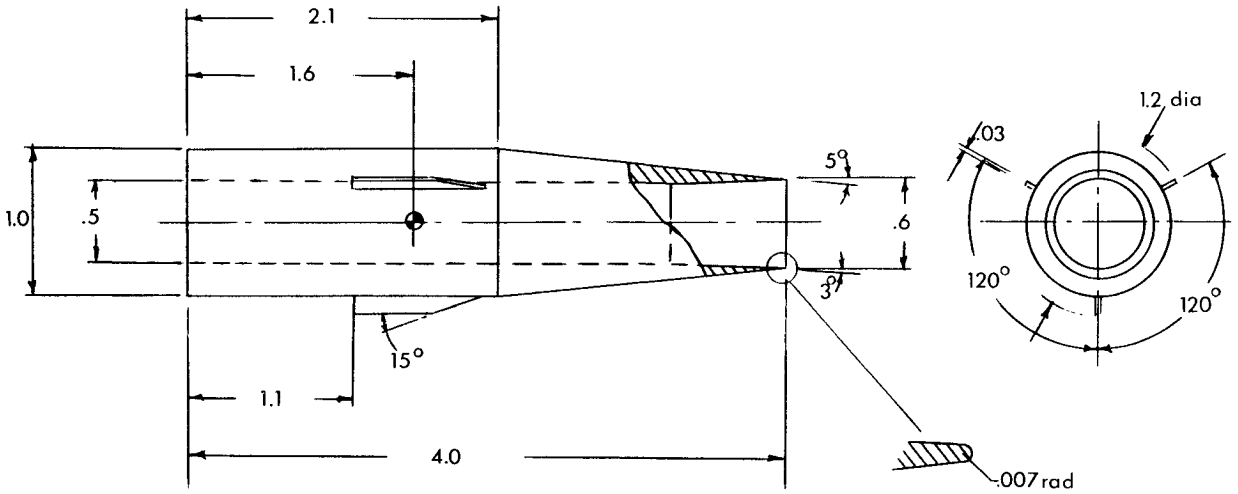

Fig. 2 Subcaliber tubular projectile—nominal dimensions.

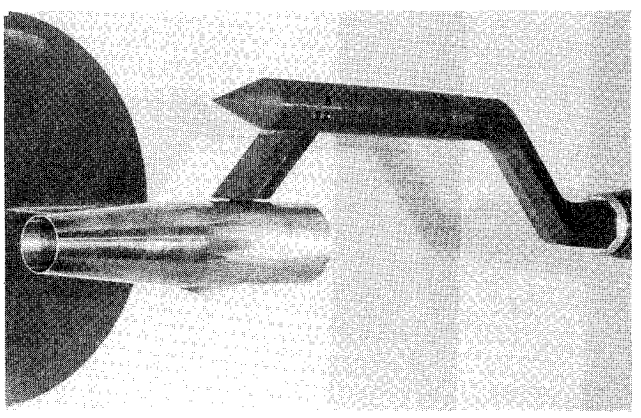

Fig. 3 Subcaliber tubular projectile and swept-strut mount in the DREV tunnel.

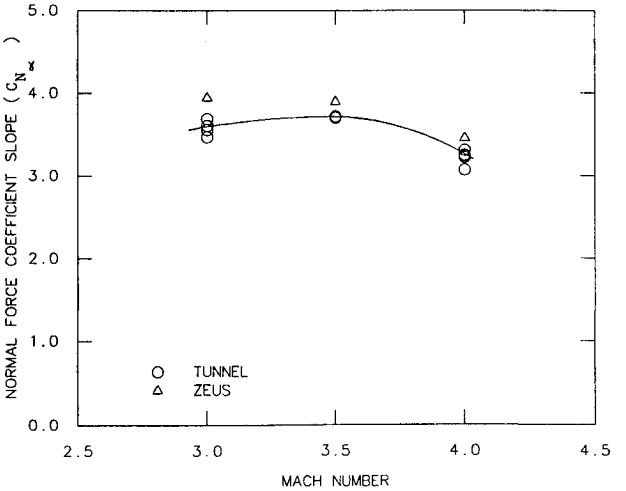

Fig. 4 Normal-force coefficient slope $C_{N\alpha}$.

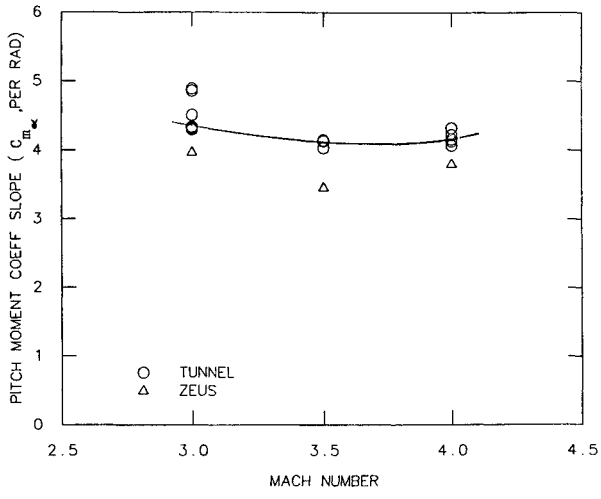

Fig. 5 Pitching-moment coefficient slope $C_{m\alpha}$ (about c.g.).

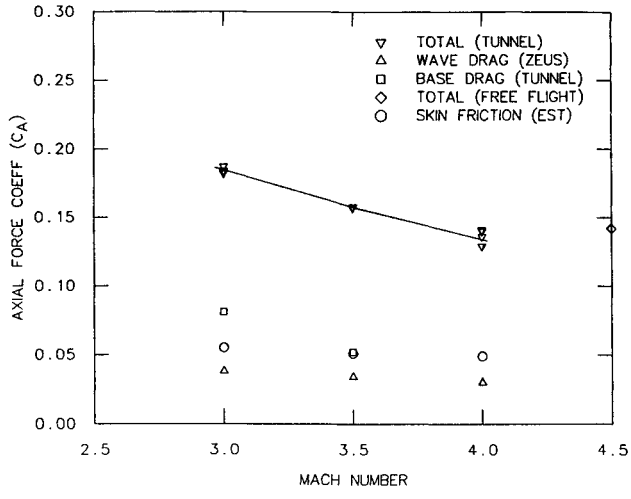

Fig. 7 Axial-force coefficient C_A.

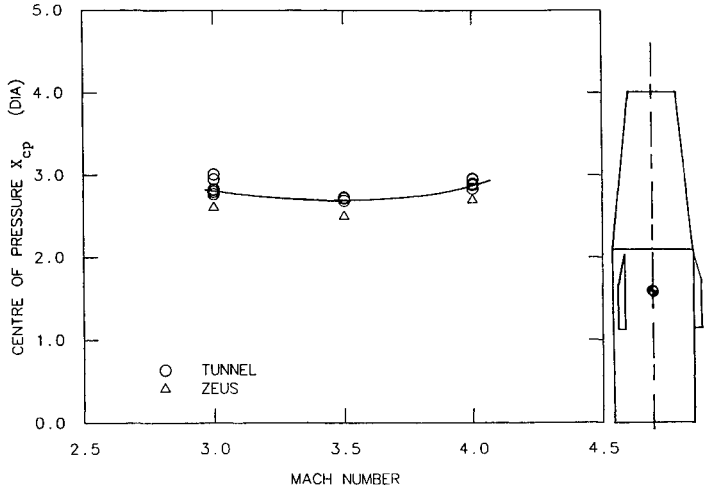

Fig. 6 Center of pressure position X_{cp} (diameters ahead of base).

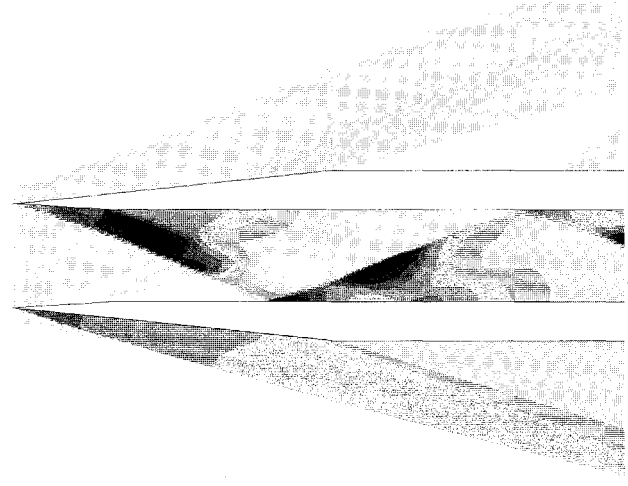

Fig. 8 Internal and external centerline pressure contours (Mach 4.0, $\alpha = 5$ deg).

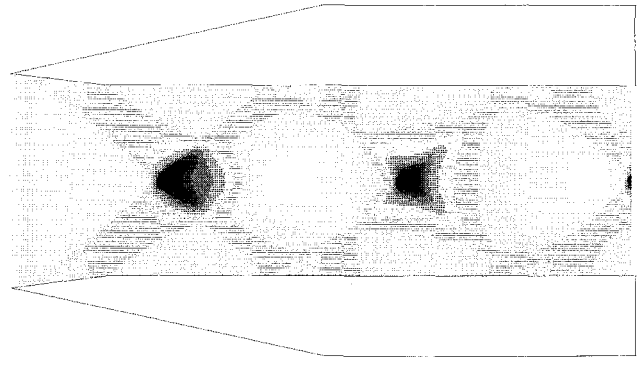

Fig. 9 Internal centerline pressure contours (Mach 4.0, $\alpha = 0$ deg; expanded vertical scale).

agreement is good, with observed differences of roughly 10% in $C_{N\alpha}$, 15% in $C_{m\alpha}$, and 0.2 diam in X_{cp}. All tunnel data have been plotted to show the run-to-run scatter. In Fig. 7, the ZEUS-calculated zero angle-of-attack wave drag is compared to both free-flight and wind-tunnel total drag. The tunnel base drag was included, as was the estimated skin-friction drag (based on wind-tunnel Reynolds number conditions of 1.7×10^6 at Mach 3.0 and 1.05×10^6 at Mach 4.0), with transition assumed to occur at 1×10^6. Base drag was unavailable at Mach 4.0. Since the ZEUS run considered zero-thickness fins, the wave drag is just body alone. Fins increased the presented area approximately 2%. The sun of the tunnel base drag, estimated skin-friction drag, and ZEUS wave drag at Mach 3.5 is roughly 15% lower than the measured tunnel total drag, and 25% lower than an extrapolated estimate of free flight. The wave drag for a conventional projectile at Mach 3.5 typically represents 50% of the total drag, while for the subcaliber tubular projectile it is shown to be approximately 25% of total.

Figure 8 is a plot showing the ZEUS-generated pressure contours (internal and external) in a vertical cutting plane along the projectile centerline at Mach 4.0 and 5-deg angle of attack. Dark regions indicate high pressure. The internal oblique shocks generated by the leading edge reflect twice down the tube creating alternating positive and negative lift. No evidence of the central small-radius body is seen. Figure 9 is a plot of the internal pressure contours to $\alpha = 0$, Mach 4.0, showing regions of higher pressure along the tube central axis where the shocks converge (expanded vertical scale). There was no evidence of a Mach reflection despite the shock convergence. Figure 10 is a contour plot of the internal pressures in a crossflow plane at a distance of 2 diam behind the nose (Mach 4.0, $\alpha = 5$ deg) showing the complex three-dimensional nature of such flows. Figure 11 is a similar plot showing pressure contours in an external crossflow plane 2.5 diam back of the nose (Mach 4.0, $\alpha = 5$ deg) in the plane of the fins. The outer boundary is the expanding oblique shock off the nose while the inner concentration of lines is the expansion wave generated at the corner. Figure 12 is a breakdown of the normal force generated by the internal and external surfaces separately at Mach 4.0 and $\alpha = 5$ deg. The alternating positive/negative lift of the inlet is clearly seen, from which one could

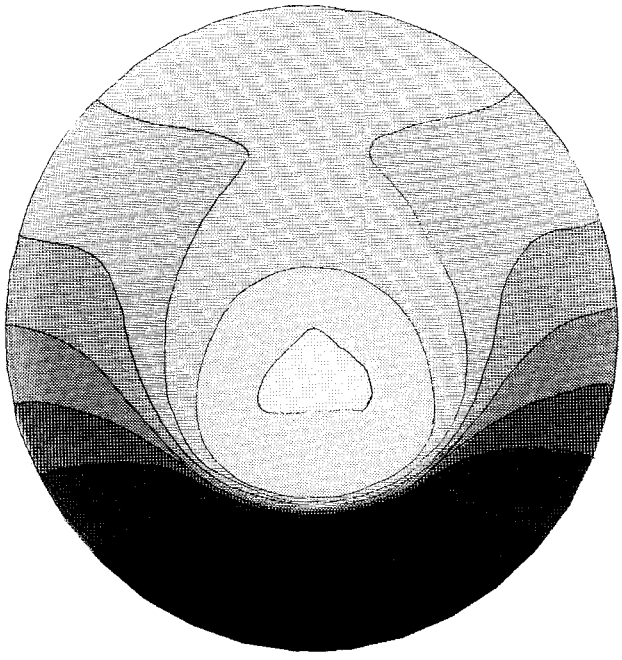

Fig. 10 Internal crossflow plane pressure contours (Mach 4.0, $\alpha = 5$ deg, $x/d = 2.0$).

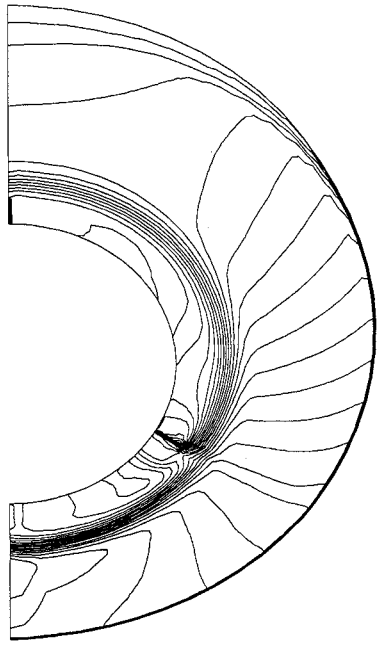

Fig. 11 External pressure contours in a crossflow plane ($x/d = 2.5$, Mach 4.0, $\alpha = 5$ deg).

predict large changes in normal force and center of pressure for small changes of tube length or Mach number.

Modeling such inlet flows with ZEUS is shown to be possible despite the inviscid flow assumption. In reality, there is a thin boundary layer along the walls that could be expected to interact with the reflecting internal shocks resulting in thickening of the boundary layer and local separation bubbles. Figure 13 from Ref. 37 illustrates the typical shock/boundary-layer interaction, the net effect of which is to shift the reflection point upstream of the inviscid position. Since no pressure data were available from the DREV tests, a further study was done using the RAE model pressure data to see if the remaining differences between tunnel and ZEUS predictions arose from shock reflection effects.

RAE Tubular Inlet—Model B

The experimental internal pressure data from the wind-tunnel tests of Ref. 8 is a further useful check on the accuracy of

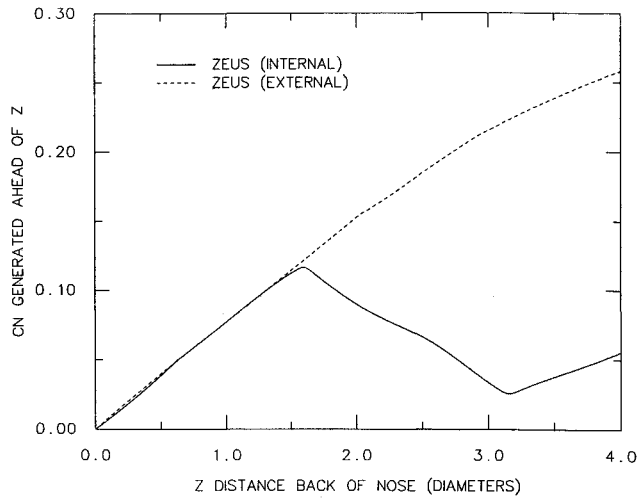

Fig. 12 Comparison of internal and external normal-force distributions (Mach 4.0, $\alpha = 5$ deg).

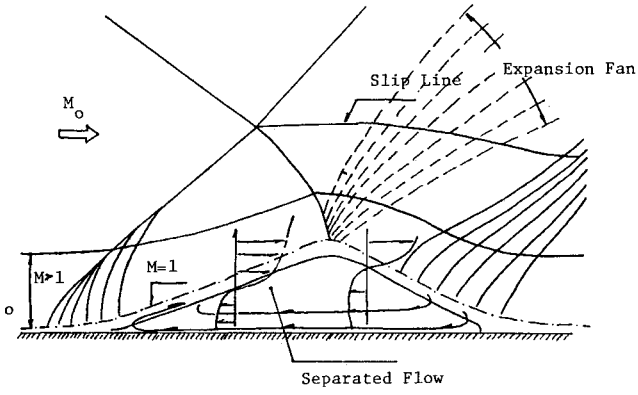

Fig. 13 Typical shock/boundary-layer interaction.[37]

the ZEUS calculations. In these tests, two lengths of circular sharp inlets were run at Mach 4 at angles of attack up to 20 deg ($l/d_t = 4.6$ and 6.9). The tube had a 10-deg inlet wedge with a throat-to-inlet diameter ratio of 0.93. Pressures were integrated and used to produce wall contour plots and lift distributions along the inner walls of the tube. The inner wall was "unwrapped" to visualize the pressure contours, and Fig. 14 shows the comparison between results of Ref. 8 and ZEUS for angles of attack of 5 and 10 deg. Good quantitative agreement it seen. Here ψ is the circumference angle with $\psi = 0$ deg being the bottom of the inlet and $\psi = 180$ deg is the top. Figure 15 shows how the normal force builds up along the inlet at $\alpha = 10$ deg. The effects of shock/boundary-layer interactions are clearly seen at the point of the second reflection, where the experimental pressures change ahead of the ZEUS result. This generates errors on the order of 0.09 in C_N at 10 deg, which translate to errors of 15–100% in total internal lift depending on the length of the tube. Since the external forces dominate for the tubular projectile (see Fig. 12), a 15% error in total lift can be accounted for in this way. ZEUS could not be expected to replicate the true damped oscillatory nature of the internal flow for longer tubes; however, runs conducted on a very long tube have shown that the pressure peaks do diminish with distance, and the net forces tend toward the slender-body theory result. ZEUS and RAE pressure contour results differ significantly along the latter part of the tube at $\alpha = 15$ deg, indicating the importance of modeling viscosity effects at angles above 10 deg.

NAE Model A

A further check on the numerical calculations was to compare ZEUS with the pressure results for the NAE Model A.[6] The Mach number range of these tests was 2.5–4.0, so extending the region of comparison between ZEUS and tunnel re-

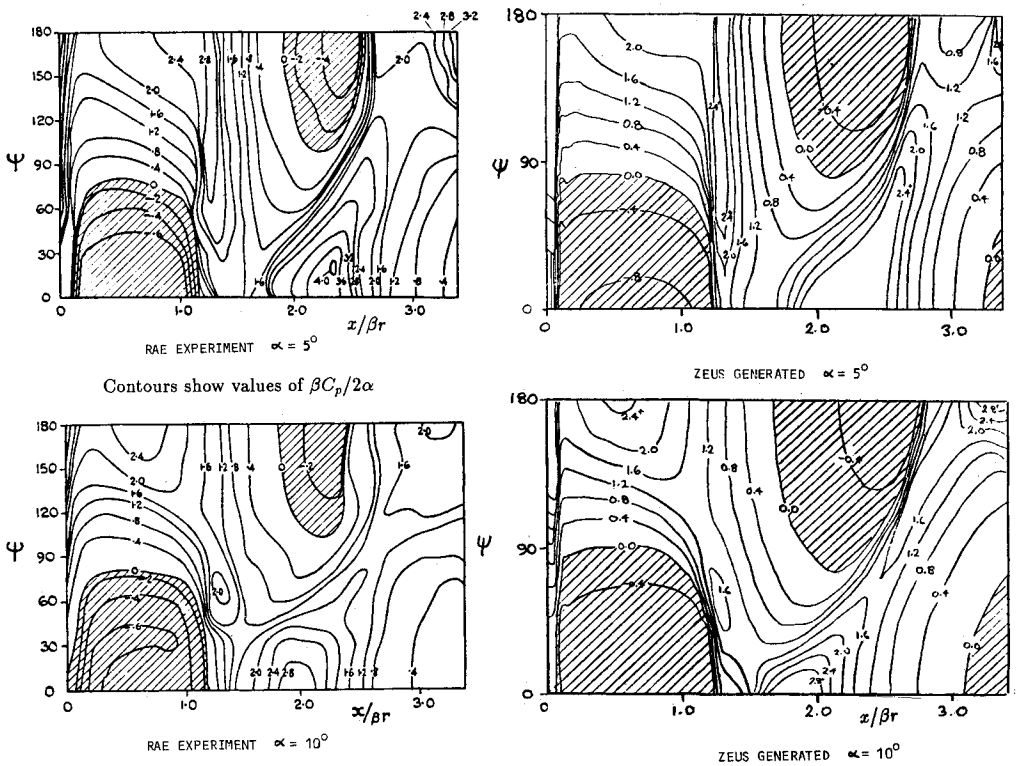

Fig. 14 Experimental and ZEUS-generated internal wall pressure contours (RAE model B).

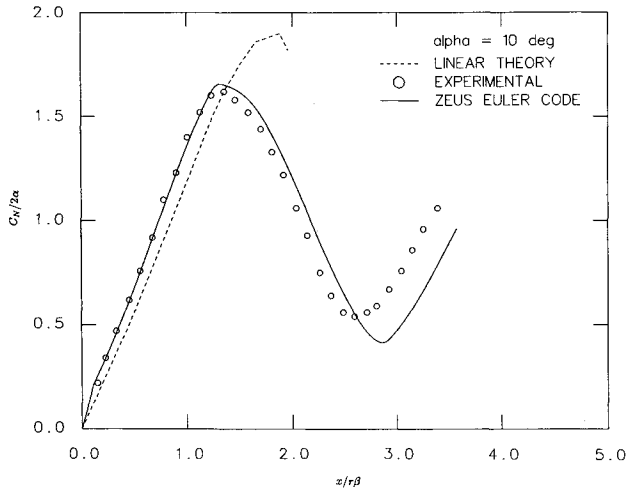

Fig. 15 Internal normal force vs duct length for RAE model B.

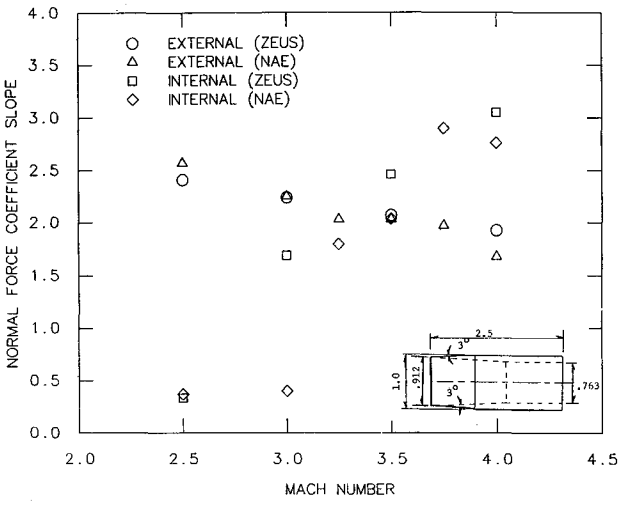

Fig. 16 NAE model A internal and external normal-force coefficient slopes C_{n_α}.

sults. Figure 16 shows the model dimensions, and shows the comparison of $C_{N\alpha}$ for both the internal and external flows. The tube is shorter than the previous test cases with an l/d_t ratio of 3.27. Agreement for the external forces is quite acceptable (14%) and is reasonable (20%) for the internal forces at all but Mach 3.0. The cause of this single discrepancy is probably the fact that the first reflection on the inner wall occurs near Mach 3, and a small error in shock position could result in large force errors.

Conclusion

It can be concluded that results from the inviscid ZEUS Euler code agree well with experimentally obtained forces, moments, and pressures on the subcaliber tubular projectile, the RAE tubular inlet, and the NAE model A. Agreement with force data on the subcaliber tubular projectile was good down to Mach 3.0, where three internal shock reflections are present. The presence of a small-radius centerbody (necessary in ZEUS) did not visibly influence the flowfield. For these test cases, the agreement for the aerodynamic coefficients was approximately: $C_{N\alpha}$ (total) = 10%, $C_{m\alpha}$ (total) = 15%, and $X_{cp} = 0.2$ diam. Accuracy of the internal normal forces predicted by ZEUS would diminish for tubes with many internal shock reflections (i.e., long tubes at low Mach numbers); however, external aerodynamic forces dominate in these cases. Shock/boundary-layer interactions cause the true internal shock reflection position to the upstream of the inviscid result, which gives rise to the errors in internal force predictions. Internal flows on tubular projectiles as angle of attack generate alternating positive and negative lift, which cause rapid changes in the center of pressure and forces with small variation of tube length or Mach number.

A swept strut was used in tunnel tests of the subcaliber tubular projectile and was shown to create minimal interference with the flowfield at Mach numbers above 2.0.

References

[1]Whitworth, J., *Miscellaneous Papers on Mechanical Subjects*, J. & J. Thomsons, London, 1858.

[2]Charters, A. C. and Thomas, R. H., "Retardation of Tubular

Projectiles Developed from 20-mm American Ball," Ballistics Research Lab., Aberdeen Proving Ground, MD, Rept. 460, April 1944.

[3]Laviolette, M. A., Cloutier, M., and Normand, M., "A Preliminary Investigation of Tubular Projectiles as a New Weapon Concept," DREV Memorandum 2037/70, Defence Research Establishment Valcartier, Quebec, Canada, Aug. 1970.

[4]D'Souza, N. and Laviolette, M. A., "Collection of Internal Flow Data from Tubular Projectiles," *Proceedings of Symposium on Internal Flows,* Subcommittee on Internal Flows, National Research Council, Ottawa, Canada, Oct. 1976.

[5]D'Souza, N., "Design and Development of 105-mm Spinning Tubular Projectile Practice Ammunition Representing APDS for Tank Guns," Space Research Corporation, Quebec, Canada, Final Rept. SRC-R-93, April 1978.

[6]Atraghji, E., "Internal and External Surface-Pressure Measurements on Three SRC Tubular Configurations in the Mach Number Range 0.8–4.0," National Aeronautical Establishment, National Research Council, Ottawa, Canada, LTR-HA-5X5/0104, Sept. 1978.

[7]Atraghji, E., "An Experimental Investigation to Study Shock Expulsion and Shock Swallowing on the 105-mm STUP," National Aeronautical Establishment, National Research Council, Ottawa, Canada, LTR-HA-5X5/0109, April 1977.

[8]Roe, P. L., "An Experimental Investigation of the Flow Through Inclined Circular Tubes at a Mach Number of 4.0," Royal Aircraft Establishment, Bedford, England, UK, TR 65110, May 1965.

[9]Cook, P. H., "Supersonic Wind-Tunnel Measurements of the Loads and Internal Pressure Distributions on Ducts at Incidence," Royal Aircraft Establishment, Bedford, England, UK, TN Aero. 1951, Feb. 1964.

[10]Cook, P. H., "Supersonic Wind-Tunnel Measurements of the Loads and Internal Pressure Distributions on Internally Parallel Ducts at Incidence," Royal Aircraft Establishment Bedford, England, TN Aero. 2962, May 1964.

[11]Flatau, A., "Tubular Projectiles—A Summary Report," Aerojet Ordnance Company, Presentation at American Defense Preparedness Association 1st Short Course on the Design of Ballistics, exact data unknown, (1985+).

[12]Nunn, R. H. and Bloomer, J. W., "Ball Obturation of a Spinning Tubular Projectile," *Journal of Spacecraft and Rockets,* Vol. 18, Nov.-Dec. 1981, pp. 533–539.

[13]Nunn, R. H. and Bry, W. A., "Drag of a Tubular Projectile with Internal Blockage," *Journal of Spacecraft and Rockets,* Vol. 21, March–April 1984, p. 216–217.

[14]Evans, J. R., Drouin, G., and Cheers, B., "Wind-Tunnel Tests of STUP Spin Damping Configurations—Trial STUPWT-1," Defence Research Establishment Valcartier, Memo 2617/83, April 1983.

[15]Evans, J. R. and Drouin, G., "Supersonic Wind-Tunnel Tests on the TP/FSDS XC-71 Subcaliber Tubular Projectile (Test Series STUPWT-4)," Defence Research Establishment Valcartier, Quebec, Canada, Memo 2861/87, Aug. 1987.

[16]Rennie, J., Dorval, M., Blanchet, A., Blanchet, G., and Mescheder, H., "Engineering Development of a 105-mm Target Practice for Fin-Stabilized-Discarding-Sabot-Tracer (TP/FSDS-T) XC-71 Ammunition," Canadian Arsenals Montreal, Canada, RDN-306-70, June 1988.

[17]Nietubicz, C. J. and Heavy, K. R., "Computational Flowfield Predictions for Ramjet and Tubular Projectiles," Proceedings of the 10th Meeting TTCP WTP-2, Vol. 1, Royal Aircraft Establishment, Bedford, England, UK, Oct. 1984, pp. 23–34.

[18]Danberg, J. E. and Sigal, A., "Evaluation of Solid-Fuel Ramjet Projectile Aerodynamic Characteristics," *Proceedings of the 13th Meeting,* TTCP WTP-2, Vol. 1, Defence Research Establishment Valcartier, Quebec, Canada, Oct. 1987, pp. 80–89.

[19]Ward, G. N., "The Approximate External and Internal Flow Past a Quasicylindrical Tube Moving at Supersonic Speeds," *Quarterly Journal of Mechanics and Applied Mathematics,* Vol. 1, P. 2, June 1948.

[20]Ward, G. N. *Linearized Theory of Steady High-Speed Flow,* Cambridge Univ. Press, Cambridge, England, UK, 1955.

[21]Lighthill, M. J., Supersonic Flow Past Bodies of Revolution," British Aeronautical Research Council, London, ARC RM 2003, Jan. 1945.

[22]Shapiro, A. H., *The Dynamics and Thermodynamics of Compressible Fluid Flow,* Vol. 1, Ronald Press, New York, 1953, pp. 147–152.

[23]Hermann, R., *Supersonic Inlet Diffusers and Introduction to Internal Aerodynamics,* Minneapolis Honeywell Regulated Company, Minneapolis, MN, 1956.

[24]D'Souza, N., Molder, S., and Moretti, G., "Numerical Method for Hypersonic Internal Flow over Blunt Leading Edges and Two Blunt Bodies," *AIAA Journal,* Vol. 10, May 1972.

[25]Politis, E., Kind, R. J., and Abdelhamid, A. N., "An Aeroprediction Method for Tubular Shapes at Supersonic Mach Numbers, Vol. 1—Analysis, and Vol. 2—User Manual," Carleton Univ., Ottawa, Canada, Final Rept. Contract 05SU3229192, Sept. 1983.

[26]Nietubicz, C. J., Pulliam, T. H., and Steger, J. L., "Numerical Solution of the Azimuthal-Invariant Thin-Layer Navier–Stokes Equations," U.S. Army Ballistic Research Lab., Aberdeen Proving Ground, MD, ARBRL-TR-02227 (AD A085716), March 1980.

[27]Nietubicz, C. J., "Navier–Stokes Computations for Conventional and Hollow Projectile Shapes at Transonic Velocities," U.S. Army Ballistic Research Lab., Aberdeen Proving Ground, MD, ARBRL-MR-03184, July 1982.

[28]Wardlaw, A. B., Jr. and Davis, S. F., "A Second-Order Godunov Method for Tactical Missiles," Naval Surface Warfare Center, White Oak, MD TR-86-506, Dec. 1986.

[29]Godunov, S. K., "A Finite-Difference Method for the Numerical Computation of Discontinuous Solutions of the Equations of Fluid Dynamics," *Mathematicheskii Sbovnik,* Vol. 47, 1959, p. 271–290.

[30]van Albada, G. D., van Leer, B., and Roberts, W. W., Jr., "A Comparative Study of Computational Methods in Cosmic Gas Dynamics," *Astronomy and Astrophysics,* Vol. 108, 1982, p. 79.

[31]Collela, P., "A Direct Eulerian MUSCL Scheme for Gas Dynamics," SIAM *Journal, Sci. Stat. Comput.,* Vol. 6, Jan. 1985, pp. 104–117.

[32]Borrel M. and Montage, J. L., "Numerical Study of a Noncentered Scheme with Application to Aerodynamics," AIAA Paper 85-1497, July 1985.

[33]Davis, S. F., "Simplified Second-Order Godunov-Type Methods," *SIAM Journal, Sci. Stat. Comput.,* Vol. 9, May 1988, pp. 445–473.

[34]Glaz, H. M. and Wardlaw, A. B., Jr., "A Higher-Order Godunov Scheme for Steady Supersonic Gas Dynamics," *Journal of Computational Physics,* Vol. No. 58, No. 2, April 1985, pp. 157–158.

[35]Murphy, G. H. and Schmidt, L. E., "The Effect of Length on the Aerodynamic Characteristics of Bodies of Revolution in Supersonic Flight," U.S. Army Ballistic Research Lab., Aberdeen Proving Ground, MD, BRL Rept. 876, 1953.

[36]Carmen, J. B., Uselton, B. L., and Winchenbach, G. L., "Wind-Tunnel and Free-Flight Range Tests of 3 and 5 Caliber Army-Navy Spinner Projectiles with Rotating Bands," Arnold Engineering Development Center, TN, AEDC TR-71-119, June 1971.

[37]"Shock-Wave Boundary-Layer Interactions," AGARD-AG-280, Feb. 1986, pp. 54.